



HAL
open science

How olive pomace can be valorized as fillers to tune the biodegradation of PHBV based composites

Sarah Lammi, Emmanuelle Gastaldi, Fabrice Gaubiac, Helene Angellier-Coussy

► To cite this version:

Sarah Lammi, Emmanuelle Gastaldi, Fabrice Gaubiac, Helene Angellier-Coussy. How olive pomace can be valorized as fillers to tune the biodegradation of PHBV based composites. *Polymer Degradation and Stability*, 2019, 166, pp.325-333. <10.1016/j.polymdegradstab.2019.06.010>. <hal-02627990>

HAL Id: hal-02627990

<https://hal.inrae.fr/hal-02627990v1>

Submitted on 25 Oct 2021

HAL is a multi-disciplinary open access archive for the deposit and dissemination of scientific research documents, whether they are published or not. The documents may come from teaching and research institutions in France or abroad, or from public or private research centers.

L'archive ouverte pluridisciplinaire HAL, est destinée au dépôt et à la diffusion de documents scientifiques de niveau recherche, publiés ou non, émanant des établissements d'enseignement et de recherche français ou étrangers, des laboratoires publics ou privés.



Distributed under a Creative Commons CC BY-NC 4.0 - Attribution - Non-commercial use - International License

25 respectively, while a biodegradation rate of only 91% was obtained after 123 days in the case
26 of neat PHBV. These results were discussed in the light of several parameters such as the
27 material structure, the affinity of the fillers for the matrix, the composition and the degree of
28 crystallinity of the filler, together with the antibacterial activity of the OP samples assessed by
29 a direct contact technique on solid medium.

30 **Keywords:** Biodegradation; biocomposites; PHBV; olive pomace; soil; packaging;
31 respirometric tests.

32 **1. Introduction**

33 Most of currently used synthetic polymers are produced from petrochemicals and are not
34 biodegradable. Persistent polymers generate long-term negative impacts on environment and
35 human health, due to their accumulation in the environment and to the diffusion of degraded
36 plastic micro- and nano-particles towards the soil, the water and finally living organisms. That
37 is why bio-sourced polymers that are fully biodegradable in natural conditions have raised
38 great interest, particularly for short-term applications such as packaging and agriculture
39 (Avérous and Pollet, 2012). It is worth noting that food packaging and agriculture sectors
40 represent the largest plastic consumption sectors, with respectively 40% and 5% of the total
41 consumption, and more than 75% of uncollectable and dispersed plastics.

42 Biodegradation is a process in which the molecular structure of materials is broken down
43 through metabolic or enzymatic mechanisms. The decomposition process occurs via enzymes
44 secreted by naturally occurring microorganisms such as bacteria, fungi or actinomycetes.

45 Biodegradation can occur in aerobic (requiring oxygen) or anaerobic (without oxygen)
46 conditions. Biomass (humus, compost) and gas (carbon dioxide and methane) are the main
47 products of a biodegradation process, carbon dioxide being generated under aerobic
48 conditions while in the case of anaerobic conditions methane was mainly produced (Andrady,

49 2011; Kumar et al., 2013; Stoleru, 2017). Besides surface properties (surface area,
50 hydrophilic/ hydrophobic properties, roughness) other intrinsic chemical and physical factors
51 are involved in the biodegradation of polymers like, first order structures (chemical structure,
52 molecular weight and molecular weight distribution) and higher order structures (glass
53 transition temperature, melting temperature, modulus of elasticity, crystallinity and crystal
54 structure) (Tokiwa et al., 2009). The degree of crystallinity is a crucial factor affecting
55 biodegradability, since enzymes mainly attack the amorphous domains of a polymer where
56 polymer chains are loosely packed, and are thus more susceptible to degradation. The
57 crystalline parts of the polymers are generally more resistant to biodegradation than the
58 amorphous ones. Aliphatic polyesters [ester bond (-CO-O-)] are typical polymers that show
59 high potential for use as biodegradable plastics, owing to their susceptibilities to lipolytic
60 enzymes and microbial degradation (Tokiwa et al., 2009).

61 Among the bio-sourced polymers able to biodegrade in natural conditions,
62 polyhydroxyalkanoates (PHAs) are a class of polyesters that present the advantage to be
63 naturally produced by a wide variety of bacteria able to accumulate from 30 to 80 % of their
64 dry weight in the form of intracellular granules as carbon and energy reserves (Madison and
65 Huisman, 1999; Singh Saharan et al., 2014). The copolymer poly(3-hydroxybutyrate-co-3-
66 hydroxyvalerate) (PHBV) is one of the most well-known PHA since already commercially
67 available for the production of disposable items and food packaging materials (Kourmentza et
68 al., 2017). However, as compared to conventional plastics, PHBV is still more expensive
69 (around 5 €/kg), which limits its use to a narrow range of applications. To decrease the overall
70 cost of materials while modulating their functional properties and maintaining their
71 biodegradability, the incorporation of lignocellulosic fillers stemming from agricultural
72 residues has become an attractive strategy (Barkoula et al., 2010; Berthet et al., 2016; Berthet
73 et al., 2017; Mousavioun et al., 2013; Lammi et al., 2018b).

74 Olive pomace (OP) is an agro-waste that has already been combined with PHBV to produce
75 biocomposites (Berthet et al., 2015; Dufresne et al., 2003; Hassaini et al., 2017; Lammi et al.,
76 2018b). OP is a solid lignocellulosic residue representing 30 to 40% of the olive oil extraction
77 by-products. It is mainly composed of skin, pulp and fragments of crushed stone (Gharbi et
78 al., 2014; Gómez-Muñoz et al., 2012). OP represents an important environmental issue mostly
79 in Mediterranean countries where they are generated in huge quantities, reaching 2,881,500
80 tons/year worldwide, in a short period of time (Ravindran and Jaiswal, 2016). Moreover, they
81 cannot be used as agricultural spreading since susceptible to cause harmful impacts on the
82 environment when let on soil. Such negative effects are mainly due to their high content in
83 phenolic and lipidic constituents, organic acid, low pH, relatively high salinity, which confer
84 them phytotoxic and antimicrobial properties. They also may be contaminated by fungi,
85 whose fungal toxins combined with polyphenolic compounds are resistant to bacterial
86 degradation, and consequently makes OP a significant source of environmental pollution
87 (Cardelli and Benitez, 1998; Gómez-Muñoz et al., 2012; Niaounakis and Halvadakis, 2004).
88 For all the above considerations related to the waste management issues generated by olive
89 pomace, there is an urgent need to explore alternatives to convert them into valuable
90 resources.

91 To date, most of available studies dealing with the incorporation of OP in polymer matrices
92 have specifically focused on the use of olive stone, which is a fraction very rich in cellulose.
93 In a previous study, it has been demonstrated that the use of either the whole OP or a pulp-
94 rich fraction, richer in lignin, could be interesting in terms of final performance of materials
95 (Lammi et al., 2018b). A better preservation of mechanical characteristics was achieved in the
96 case of pulp-rich filler (PF), due to better filler/matrix interactions and hence higher
97 interfacial adhesion. A range of water vapor and oxygen permeabilities could be reached,
98 which makes it possible to consider the use of OP-based biocomposites as food packaging

99 (rigid trays) for various types of food products, but also for horticulture applications.
100 However, it has never been checked if the presence of lignin could have a negative impact on
101 the biodegradability of resulting composite materials.

102 In this context, the objective of the present work is to investigate for the first time the impact
103 of the composition of OP fillers on the capability of PHBV/OP-based biocomposites to
104 biodegrade in soil. This is of prime importance since such materials are intended to be used to
105 short-term use applications, such as pots or trays. For that purpose, three types of fillers
106 displaying contrasted biochemical composition have been produced by following a dry
107 fractionation process already reported by Lammi et al., 2018a, *i.e.* a stone-rich filler, a pulp-
108 rich filler and a filler produced from the whole OP residue. PHBV/OP-based biocomposites
109 were prepared by thermomolding, with filler content up to 15 wt%. Biodegradation was
110 evaluated through respirometric tests conducted in soil, at 28°C and in aerobic conditions
111 during 4 months. The biodegradation rate of the different OP fractions and the resulting
112 PHBV-based composites was discussed in relation to the material structure, as well as to the
113 antibacterial activity of the OP samples assessed by a direct contact technique on solid
114 medium.

115 **2. Materials and methods**

116 **2.1. Materials**

117 Olive pomace (OP) was kindly supplied by a local olive producer in the region of Azeffoun
118 (Tizi-Ouzou, north-center of Algeria). It was obtained from the olive oil extraction of the
119 *Chemlal* variety. Raw olive pomace was dried in an oven at 60°C for 24 hours before further
120 usage.

121 A commercial grade of polyhydroxy-(butyrate-co-valerate) (PHBV) containing 3% of valerate
122 was purchased from NaturePlast (France) in the form of pellets (PHI002 grade).

123 Sulfuric acid, arabinose, xylose and glucose (Sigma-Aldrich), formamide, diiodomethane
124 (Acros Organics, Geel, Belgium), ethylene glycol (Aldrich chemical Co. Inc., Milwaukee,
125 USA) and glycerol (Merck, Darmstadt, Germany) were used for characterization of OP fillers.
126 Barium chloride-Dihydrat (VWR Chemicals, Germany), sodium hydroxide (Grosseron,
127 France), thymolphtalein (Alfa Aesar, Germany), hydrochloric acid and microcrystalline
128 cellulose (Merck, Germany) were used for biodegradation tests.

129 **2.2. Preparation and characterization of olive pomace-based fillers**

130 Pulp-rich and stone-rich fractions were isolated from the raw olive pomace sample by dry
131 fractionation with friction solicitations in a ball mill, as described by Lammi et al. (2018a).
132 resulting fractions were then sieved and reduced in size using successive dry grinding steps
133 (Lammi et al., 2018a). The obtained powders, *i.e.* the pulp-rich fraction (PF), the stone-rich
134 fraction (SF) and the crude OP fraction (F0), displayed a median apparent diameter of
135 respectively 55, 59 and 85 μm (Lammi et al., 2018b).

136 The cellulose, hemicellulose and lignin contents of OP-based fillers were characterized in a
137 two-stage acid hydrolysis. The first hydrolysis was carried out using a 72 wt% H_2SO_4 solution
138 at 30°C for 1 hour, while the second one was performed using a 4 wt% H_2SO_4 solution at
139 121°C for 1 hour following the protocol described by Barakat et al. (2014). The lignin content
140 was determined by the Klason method (Nicholson et al., 2014). The protein content was
141 estimated according to the formula ($\text{N} \times 6.25$) (Jones, 1941), after the determination of
142 nitrogen content (N) by elementary analysis. The moisture content was determined by drying
143 about two grams of sample in an oven at 110°C until reaching weight equilibrium. The ashes
144 content was obtained by igniting about one gram of sample in a muffle furnace at 600°C for 5
145 hours. pH measurements were carried out with a pH electrode (VWR 1100L, Germany) on an
146 aqueous suspension (five grams of sample mixed with 50 mL of distilled water) put under

147 magnetic stirring during 30 min (Haddadin et al., 2009). All the analyses were performed in
148 triplicate.

149 **2.3. Preparation and characterization of OP/PHBV-based biocomposites**

150 PHBV pellets and OP-based fillers (15 wt%) were blended in a HAAKE Rheomix internal
151 mixer operating at a rotor speed of 60 rpm and 170°C during 5 min. Obtained compounds
152 were cooled to room temperature and then, ground in a knife mill (SM 300, Retch, Germany)
153 at a speed of 2200 rpm through a 4 mm grid to obtain composite pellets. Compounds were
154 dried at 60°C for at least 8 hours before the preparation of materials. Biocomposite films
155 (10.5 cm wide squares, average thickness about 250 µm) were prepared by hot pressing the
156 pellets between two Teflon coated plates at 170°C, using a hydraulic thermopress (PLM 10 T,
157 Techmo, Nazelles, France). Samples were first allowed to melt for 3 min. Then, a pressure of
158 150 bars was applied for 2 min. The films were cooled at room temperature before being
159 removed from the mould.

160 The percentage of carbon of OP fillers, neat PHBV, biocomposites and microcrystalline
161 cellulose was determined using an elemental analyzer Vario Micro Cube (Elementar,
162 Germany).

163 The surface morphology of the OP-fillers and the cross-section of the PHBV-based films
164 (obtained after cryo-fracturing under liquid nitrogen) were observed by scanning electron
165 microscopy (SEM) using a scanning electron microscope (SEM S-4500, Hitachi, Japan) with
166 an acceleration voltage of 2 kV and a detector for secondary electrons. The samples were
167 previously coated with gold/palladium by ion beam sputtering.

168 Antibacterial tests were carried out to evaluate the antibacterial effect of both fillers and
169 composites films following the direct contact technique on Mueller-Hinton agar against two

170 selected bacterial strains (*Staphylococcus aureus* CIP 53156 and *Escherichia coli* 55B5 CIP
171 52170). The tests were performed on young pre-cultures of both bacteria in a Mueller-Hinton
172 broth. Bacterial suspensions turbidity was standardized to 0.5 McFarland. The OP-based
173 fillers (in the form of powders) were deposited in wells of 10 mm in diameter obtained with a
174 piece-cutter on the agar medium. In the case of materials, discs of 10 mm diameter pre-cut
175 from the composite films were putted on the surface of the agar previously inoculated with the
176 target bacteria. The incubation of Petri dishes was carried out at 30°C for 24 hours. The
177 occurrence of an antibacterial effect of both materials was evidenced by the appearance a
178 clear inhibition zone around the wells/discs.

179 **2.4. Biodegradation tests**

180 Respirometric tests were conducted in aerobic conditions to evaluate the biodegradation rate
181 of OP-based fillers, PHBV matrix and PHBV/OP based biocomposites in soil medium. The
182 method was adapted from the US standard ASTM D5988-96, which is a Standard Test
183 Method for Determining Aerobic Biodegradation in Soil of Plastic Materials. The released
184 CO₂ being proportional to the percentage of biodegraded substrate, the CO₂ evolution
185 measures ultimate degradation (*i.e.* mineralization) in which a substance is broken down to its
186 final products. Beforehand, film samples were frozen under liquid nitrogen and then ground
187 with a domestic grinder (Moulinex type DPA1, France) to obtain particles around 1–2 mm.

188 The soil used in this study was taken from the park of the University of Montpellier (France)
189 in April 2017, after removal of the superficial vegetation layer. The big pebbles and foreign
190 objects were removed manually to obtain a homogeneous sample. The soil was dried in open
191 air for one week and then sieved through a 2 mm mesh. The total dry solids content was
192 determined by drying the soil at 105 °C until a constant weight. Soil characteristics were as
193 follows: pH 6.8 (H₂O), 2.3 wt% of organic matter, 16.85 wt% of clay, 26.85 wt% of lime and
194 56.3 wt% of sand.

195 Biodegradation tests were carried out in cylindrical hermetic glass vessels (1000 mL capacity)
196 containing three small open polypropylene flasks (60 mL capacity) as described by Chevillard
197 et al. (2012). The first flask contained 25 g of dry soil mixed with samples whose weight
198 corresponded to 50 mg of carbon. The water content of soil samples was adjusted to reach
199 80% of the soil water retention capacity (410 μ l/g wet basis). The second flask contained 10
200 mL NaOH solution (0.1 M) to trap the CO₂ produced by microorganisms. The third flask
201 contained distilled water, in order to maintain the relative humidity at 100% inside the vessel.
202 The glass vessels were hermetically closed and incubated in the dark at 28 \pm 1°C. Every
203 week, glass vessels were open to ensure the back titration of the excess of NaOH, which has
204 not reacted with CO₂. Before titrating the residual NaOH with HCl solution (0.1 M) in the
205 presence of thymophthaleine 0.10% (prepared in ethanol 95.5% (v/v)), 5 mL of barium
206 chloride solution (20% (w/v) in water) were added in each flask to precipitate carbonate ions.
207 The flasks containing soil were weighted and appropriate amount of water was added in order
208 to keep constant the water content initially fixed at 80% of the soil water retention capacity.
209 During this procedure, the glass vessels were left open during 2 min in order to be aerated. At
210 each dosage, a new flask containing 10 mL NaOH (0.1 M) was placed in each glass vessel
211 before being closed and put in the dark at 28°C until the next measurement. Biodegradation
212 experiments included control and blank samples. The control samples were microcrystalline
213 cellulose, a positive reference material well known for its biodegradation properties. The
214 blank samples corresponded to the soil alone, without any addition of an external carbon
215 source to measure both the CO₂ produced by the soil carbon substrate and the CO₂ present in
216 the air of the glass vessel. All experiments were run in triplicate.
217 Results were calculated by subtracting the CO₂ production of the blank. The theoretical
218 maximum CO₂ potential (CO₂ _{max} (mg)) produced by total oxidation of the material is
219 calculated using the following equation:

220
$$CO_{2\max} = C \times \frac{44.01}{12.01} \text{ (equation 1)}$$

221 Where C is the amount of carbon of the sample introduced in the soil for the test (mg).

222 The percentage of biodegradation (B) is calculated by equation (2):

223
$$B = \frac{CO_2 \text{ material} - CO_2 \text{ blank}}{CO_2 \text{ max}} \text{ (equation 2)}$$

224 As required by the ASTM D5988-96 standard, cellulose is used as a reference substance in
225 order to check the activity of the soil and its biodegradation percentage should be higher than
226 70 % after six months. Otherwise, the test must be regarded as invalid and should be repeated
227 using another fresh soil.

228 The experimental degradation data were modeled with the Hill equation:

229
$$Deg = Deg_{max} \cdot \frac{t^n}{(k^n + t^n)} \text{ (equation 3)}$$

230 where Deg [%] is the percentage of degradation at time t [days], Degmax [%] the percentage
231 of degradation at infinite time, k [days], the time for which $Deg = \frac{1}{2} Deg_{max}$ and n the curve
232 radius of the sigmoid function.

233 **3. Results and discussion**

234 **3.1. Biodegradability of OP-based fillers**

235 Respirometric tests were used to evaluate the degree and rate of aerobic biodegradation of
236 OP-based fillers and related PHBV composites in contact with soil. CO₂ evolution provides
237 an indicator of the ultimate biodegradability ascribed to the mineralization of the test samples.
238 The biodegradation kinetic of the three OP-based fillers and corresponding Hill parameters
239 are presented in Figure 1 and Table 1, respectively. Respirometric tests conducted in the
240 present study were validated since the biodegradation rate of micronized cellulose selected
241 here as a reference material, reached 70% after only 45 days, while this threshold should be

242 obtained in less than 183 days (6 months) to consider the test as valid according to the
243 requirements of ASTM D5988-96 standard.

244 The characteristic Hill sigmoidal shape of the biodegradation curves is known to reflect the
245 two phases commonly ascribed to the polymer degradation process involving
246 microorganisms. Firstly, the polymer chains are cleaved in small fragments due the action of
247 extracellular enzymes, and then, these latter are transported into the cell where they are
248 ultimately mineralized mainly in CO₂, water vapour, minerals, and biomass (Bastiolli, 2005).

249 As compared to cellulose known to rapidly biodegrade in soil, all the OP-based fillers
250 biodegraded rather well, ranking as follows F0<SF<PF, with a biodegradation threshold
251 superior to 70% (relative to cellulose) reached in 65, 43 and 37 days respectively. As
252 evidenced in Table 1, they all reached their rate of maximal degradation ($\text{Time}_{\text{rate max}}$) in less
253 than 20 days, and it took less than 6 months for F0 and SF samples to reach 50% of Deg_{max} as
254 indicated by k values. Regarding the pulp-rich fraction (PF), which exhibited the highest
255 maximum rate of biodegradation (with a $\text{Deg}_{\text{rate max}}$ value twice higher than these observed for
256 the two others fillers), it is worth noting that this sample displayed a peculiar biodegradation
257 curve shape reflected by a low radius of the sigmoid function.

258 **Figure 1.**

259 **Table 1.**

260 The biodegradation curve of the stone-rich fraction (SF) was almost superimposed on that of
261 the cellulose reference, which could be ascribed to its richer cellulose content as compared to
262 the other fillers (around 10, 12 and 17% for PF, F0 and SF respectively) (Table 2). Contrary
263 to our expectations, the highest rate of biodegradation was recorded for the pulp-rich sample
264 (PF), despite its highest lignin content (48.9 wt%) as compared to F0 (44.2 wt%) and SF (37.7
265 wt%) samples (Table 2). Indeed, lignin is a complex polyphenolic polymer that is known for

266 its resistance to microbial degradation (Dashtban et al., 2010; Singh et al., 2016; Taherzadeh
267 and Karimi, 2008). Furthermore, the biodegradation rate of organic substances was
268 demonstrated to follow this order: carbohydrates > hemicellulose > cellulose > lignin
269 (Cooperband, 2002). In addition, as already evidenced by contact angle measurements
270 (Lammi et al., 2018b), lignin was shown to confer a greater hydrophobicity to the PF fraction
271 compared to the other OP-based ones. Thus, the hydrophobic character of PF should
272 theoretically have reduced its affinity for soil water and therefore its contact with
273 microorganisms. As a consequence, another reason is here proposed to explain the highest
274 biodegradation rate displayed by the pulp-rich fraction (PF), related to the higher protein
275 content of PF (8.7%) than the one of F0 (4.9%) and SF (0.6%) (Table 2). Recent researches
276 have highlighted that factors such as organic carbon (C), nitrogen (N) content and carbon to
277 nitrogen ratio (C/N) could be key elements to improve the biodegradation process, since they
278 ensure optimal conditions for the growth and development of microbial communities involved
279 in the decomposition of organic matter (De Bertoldi et al., 1983; Muktadirul Bari Chowdhury
280 et al., 2013). Indeed, the optimal C/N ratio generally found in a compost medium ranged from
281 25 to 35, since it is assumed that microorganisms require 30 parts of C per unit of N for the
282 composting process. Medium exhibiting high C/N ratios are known to delay the composting
283 process due to a surplus of degradable substrate for the microorganisms (Bishop Godfrey,
284 1983). In the soil medium used in the present study, SF sample exhibited a C/N ratio of about
285 55 against 37 and 65 for PF and F0 respectively (Table 2), which may explain the fact that
286 PF biodegraded at a higher rate than F0 and SF.

287 Given that the crude OP sample (F0) consisted of a mixture of the pulp and stone tissues,
288 composed of about 31% of PF and 56% of SF (Table 2), it was expected to display an
289 intermediate biodegradation kinetic. However, results showed that F0 exhibited a slower
290 biodegradation rate than these two fractions. It is worth noting that all the samples underwent

291 the same grinding route in such a way to obtain similar average particle sizes (Lammi et al.,
292 2018b) (Figure 2). The slow biodegradation kinetic of F0 was probably due to a more
293 complex organization of the lignocellulosic structure within the particles, making them less
294 accessible to the soil microorganisms, as compared to the two other pure and contrasted
295 fractions (PF and SF). As reported by Taherzadeh and Karimi (2008), lignin and
296 hemicellulose contents could also influence the accessibility of surface for enzymatic attack.
297 In the same context, Mais et al. (2002) indicated that milling could be employed to alter the
298 inherent ultra-structure of lignocellulose and decrease the degree of crystallinity, and
299 suggested that reducing the size of the material by milling would make it more amenable to
300 enzymatic degradation. However, this hypothesis would deserve to be further explored and
301 validated through crystallinity measurements since, in the present study, the physical
302 treatments applied to mill the pomace fractions were probably too superficial and mild to
303 induce such structural changes.

304 **Figure 2.**

305 **Table 2.**

306 After 123 days, the biodegradation rates reached 88.6, 111.8, 117.2 and 162.8% for F0,
307 cellulose, SF and PF samples respectively (Figure 1A). Reaching biodegradation rate higher
308 than 100% has already been reported and is known as priming effect. It generally occurs when
309 the soil inoculum of the test reactor containing the samples produces more CO₂ than the soil
310 inoculum in the blank reactors. This peculiar behavior results from a stimulation of the
311 organic matter mineralization due to easily decomposable organic matter that would be
312 released in the medium during the biodegradation of specific materials. This phenomenon
313 would arise from particular interactions occurring between the transformation of the added
314 substances and the natural soil cycle of carbon (Kuzyakov et al., 2000).

315 Based on our results, the biodegradation patterns of the OP-fillers (Figure 1A) did not support
316 the different literature data reporting that crude olive pomace would be unable to biodegrade
317 in soil, being consequently at the origin of environmental pollution. According to Cardoso et
318 al. (2005), the phenolic compounds being not degraded during olive oil extraction, olive
319 pomace, like olive pulp, would be expected to be a good source of those compounds.

320 To verify this assumption, antibiogram tests have been conducted on the OP-based fillers
321 using two targeted bacterial strains (*S. aureus* and *E. coli*). No antibacterial activity was
322 evidenced, as clearly shown in Figure 3 by the absence of bacterial growth inhibition zone
323 around the wells of the different samples. The dark color was due to the diffusion of
324 chlorophyll pigments in Mueller-Hinton agar. These pigments responsible for the olive fruit
325 color were more concentrated in the particles of F0 and PF powders, as already demonstrated
326 by Lammi et al. (2018a). Even if these results appeared rather unexpected with respect to
327 literature, they underpinned our biodegradation results. To explain the lack of antibacterial
328 effect, it could be assumed that the preliminary stage consisting in the drying of the raw
329 biomass for 24 hours at 60°C would cause a thermal denaturation of the active compounds
330 resulting in a loss of any expected inhibiting effect. In addition, during the successive
331 grinding operations, the various OP-based samples were exposed to frictional heating when in
332 contact with grinder. Exposure to such a temperature increase would also contribute to
333 denature the bioactive substances involved in the targeted antibacterial effect. To finish with,
334 it cannot be excluded that the OP-based fillers were also probably already microbiologically
335 contaminated. This contamination could occur after the drying of the crude pomace or during
336 the grinding and sieving operations, both stages being done at room temperature in contact
337 with the ambient air. These microorganisms might enhance the biodegradation of the OP-
338 based fillers acting in cooperation with the soil microorganisms, both contributing to a faster
339 biodegradation rate.

340 **Figure 3.**

341 **3.2. Biodegradability of OP-based biocomposites**

342 The biodegradation kinetic of neat PHBV and OP/PHBV-based composites are presented in
343 Figure 4, and the respective Hill's parameters obtained by modeling experimental data
344 according to Hill equation are gathered in Table 1.

345 Neat PHBV exhibited slower degradation kinetic than OP/PHBV-based composites whatever
346 the OP fraction used as filler. Hill's parameters clearly confirmed that incorporation of OP
347 fillers up to 15wt% in PHBV accelerated the biodegradation of the composite materials
348 compared to the neat polymer. As indicated in Table 1, this latter recorded only 163% of
349 degradation at infinite time and reached 50% (k) of this degradation after about 109 days. By
350 contrast, all the OP-based composites exceeded 200%, with k values being reached in less
351 than 85 days. It is interesting to note that the nature of the filler used had no significant
352 influence on the degradation profile of composites. In fact, the neat PHBV matrix recorded
353 the lowest rate of degradation with a maximum ($\text{Deg}_{\text{rate max}}$) reached after 95 days ($\text{Time}_{\text{rate}}$
354 $_{\text{max}}$) whereas all the composite formulations displayed twice the maximum degradation rate
355 after only 68 days (Table 1).

356 Finally, 4 months of incubation at 28°C in the soil and under aerobic conditions, PHBV
357 biodegradation reached 91% (*i.e.* about 83% relative to cellulose) without attaining the
358 plateau of carbon dioxide released. This indicated that respirometric measurements should
359 have been prolonged a few months more for PHBV without however questioning its
360 biodegradability in soil. As claimed by the recent specification standard NF EN 17033, a
361 biodegradation level of 90% relative to cellulose should be reached no later than 2 years.
362 According to Boopathy (2000), biodegradation is dependent on a number of factors such as
363 microbial activity of the environment, exposed surface area, temperature, pH and molecular

364 weight. It is worth specifying that in the present study all the material samples were
365 previously ground as particles around 1–2 mm before being tested. As a consequence, it could
366 be attested that all the respirometric tests have been performed in the same standardized
367 conditions, the results obtained being therefore comparable.

368 To conclude, the PHBV-based biocomposites could be considered as significantly much more
369 biodegradable than the virgin PHBV matrix whatever the OP fractions used. Monitoring the
370 evolution of the carbon dioxide over time through respirometric revealed that the
371 biodegradation kinetics of the biocomposite materials followed the order: PHBV<PHBV-
372 PF<PHBV-SF<PHBV-F0. After 123 days of soil incubation, PHBV-PF and PHBV-SF
373 formulations overpassed 134% of biodegradation, and the PHBV-F0 film exceeded 143%.
374 This peculiar behavior resulted from the priming effect already mentioned above for the OP-
375 fractions which all reached biodegradation rates greater than 100%. This synergistic effect
376 was certainly related to the presence of OP-fillers, which further boost the biodegradation
377 process of the composites compared to the PHBV matrix alone. Biodegradation rates of
378 biocomposites exceeding 100% have already been reported for films made of gliadins cross-
379 linked by cinnamaldehyde (Balaguer et al., 2015), starch-polystyrene foams (Pushpadass et
380 al., 2010), or L-poly lactide-polycaprolactone co-polymer films (Plackett, 2006) under
381 composting conditions.

382 **Figure 4.**

383 The increased biodegradability of composite materials might be the result of three
384 concomitant effects. Firstly, it could be due to the increased hydrophilicity of biocomposites
385 compared to virgin PHBV due to the incorporation of fillers that are much more hydrophilic
386 than the matrix. This assumption was supported by results reported by Lammi et al. (2018b)
387 indicating a significant increase of the water vapor permeability of PHBV films after

388 introducing OP-fillers, and especially in the case of F0 and SF fractions. A higher
389 hydrophilicity would favor the adsorption and then the transport of water within the
390 composite material, which in turn would promote the microbial degradation of material
391 (Chevillard et al., 2012).

392 Secondly, differences in biodegradation patterns between composite materials could be
393 attributed to differences in the microstructure of materials. A poor affinity between the filler
394 and the polymer matrix would result in a poor dispersion of the fillers and the formation of
395 aggregates as well as a poor filler/matrix adhesion that would induce the creation of voids
396 between the filler and the matrix. These two phenomena would lead to the creation of a bulk
397 porosity and therefore to the creation of a preferential pathway for the transport of water
398 within the composite material. Such microstructural defects would also be prone to increase
399 the fragility of materials favoring their physical disintegration, and thus resulting in a higher
400 contact surface for ensuring microorganisms colonization. This hypothesis was supported by
401 the microstructural investigation of the composite materials characterized by SEM after cryo-
402 fracture (Figure 5). Although PHBV cross-section displayed a homogeneous and smooth
403 surface, contrariwise, the cross sections of PHBV-F0 and PHBV-SF films were rough, with
404 the evidence of cracks and voids at the filler/matrix interface probably due to the debonding
405 of fillers. As described above, this would allow microorganisms to attach and form biofilms
406 colonizing the material surface. In the case of PHBV/PF composites, the particles were
407 entirely wetted by the polymer matrix, indicating a good filler/matrix interfacial adhesion.
408 This was attributed to the great affinity between PF fillers and PHBV matrix as confirmed by
409 similar values of surface energy, previously demonstrated (Lammi et al., 2018b). This more
410 homogenous and compact microstructure would hinder the diffusion of water and thus the
411 accessibility to microorganisms, as compared to PHBV/F0 and PHBV/SF composites. As a

412 consequence, PHBV-PF composite material biodegraded at a lower rate than the two other
413 composites containing F0 and SF fillers.

414 **Figure 5.**

415 Difference in crystallinity between the materials might also be at the origin of changes in their
416 biodegradation patterns. Indeed, the kinetic of enzymatic degradation is known to depend on
417 the overall crystallinity of the material (El-Hadi et al., 2002). An increase in polymer
418 crystallinity is known to be detrimental for the polymer biodegradability since crystalline
419 zones are less accessible for the microorganisms (Wei et al., 2015). Indeed, as previously
420 demonstrated by the authors Lammi et al. (2018b), the presence of F0 and SF as fillers in the
421 PHBV led to a decrease in the crystallinity degree (X_c) of the neat matrix whereas the
422 crystallinity of the PHBV/PF was increased. The recorded degrees of crystallinity X_c (%)
423 were 65, 68, 75 and 78% for PHBV-F0, PHBV-SF, PHBV and PHBV-PF films, respectively
424 (Lammi et al., 2018b). Such an anti-nucleating effect might contribute to facilitate the
425 biodegradability of PHBV/F0 and PHBV/SF composites as compared to PHBV/PF. This
426 phenomenon was previously observed for biocomposites based on polyhydroxybutyrate and
427 fermentation residue coming from potato peel waste (Wei et al., 2015). In the case of the
428 PHBV/PF composite formulation, it is worth noting that the effect of the increased
429 crystallinity was compensated by the opposite effect resulting from the increased
430 hydrophilicity and the more heterogenous microstructure as compared to the neat PHBV
431 matrix.

432 Finally, biodegradation performance of all the composite materials was underpinned by the
433 antibiogram tests undertaken on composite films and neat PHBV chosen as control. As shown
434 in Figure 3, no inhibition zone was evidenced around the different disks, which was in full
435 agreement with their fast biodegradation in the soil medium. Such positive results enabled to

436 envisage other routes for valorizing the different fractions stemming from olive pomace
437 wastes and justified the approach consisting in introducing them as fillers for developing
438 biodegradable composites based on PHBV.

439 **4. Conclusion**

440 The present work fits into a larger environmental context aiming at reducing the impact of the
441 agro-residues by valorising them to design biodegradable materials. With a view to achieve a
442 complete valorisation of olive pomace, all its components (including the constitutive tissues
443 of the olive fruit, namely the pulp and the stone) were transformed in powders using a
444 rationale dry fractionation process before being used as fillers to develop PHBV-based
445 biocomposites. The impact of such fillers on the biodegradability in soil of the resulting
446 composite materials was investigated in relation with their respective chemical composition.
447 Results revealed that the incorporation of OP-based fillers in PHBV accelerated the
448 biodegradation kinetics of the composites, which exceeded 100% after 4 months. These
449 results were supported by measurements of crystallinity as well as SEM observations.
450 Moreover, the absence of any antibacterial effect of both the olive pomace-based fillers and
451 the resulting biocomposites towards the target bacteria (*Staphylococcus aureus* and
452 *Escherichia coli*) confirmed the capability of such materials to biodegrade in soil and fully
453 justified the relevance of this study. To conclude, this research presented a promising track for
454 the valorisation of olive pomace through the elaboration of biocomposites materials that
455 might be notably intended for short-term use such as packaging.

456 on the other hand, these results clearly showed the interest of crude OP fractionation and led
457 us to propose another exploitation field for the SF and PF fractions as natural and
458 biodegradable fertilizers for the agricultural grounds.

459 **Acknowledgments**

460 This research was supported by MALICE project co-financed by the European Regional
461 Development Fund, and the PNE Program (2016–2017) of the Algerian Ministry of Higher
462 Education and Scientific Research.

463 **References**

- 464 • Andrady AL. Microplastics in the marine environment: A review. *Marine Pollution*
465 *Bulletin*, 2011; 62:1596–1605. DOI:10.1016.
- 466 • Avérous L, Pollet E. Chapter 2: Biodegradable Polymers. *Environmental Silicate Nano-*
467 *Biocomposites, Green Energy and Technology*, DOI: 10.1007/978-1-4471-4108-2-2,
468 ©Springer-Verlag London, 2012.
- 469 • Balaguer MP, Villanova J, Cesar G, Gavara R, Hernandez-Munoz P. Compostable
470 properties of antimicrobial bioplastics based on cinnamaldehyde cross-linked gliadins.
471 *Chemical Engineering Journal*, 2015; 262: 447–455.
- 472 • Barakat A, Chuetor S, Monlau F, Solhy A, Rouau X. Eco-friendly dry chemo-mechanical
473 pretreatments of lignocellulosic biomass: Impact on energy and yield of the enzymatic
474 hydrolysis. *Applied Energy*, 2014; 113: 97–105.
- 475 • Barkoula NM, Garkhail SK, Peijs T. Biodegradable composites based on
476 flax/polyhydroxybutyrate and its copolymer with hydroxyvalerate. *Industrial Crops and*
477 *Products*, 2010; 31: 34–42.
- 478 • Bastioli C. *Handbook of biodegradable polymers*. Smithers Rapra Technology;2005.
- 479 • Berthet MA, Angellier-Coussy H, Guillard V, Gontard N. Vegetal fibre-based
480 biocomposites: Which stakes for food packaging applications. *Journal of Applied Polymer*
481 *Science*, 2016;133(2), SI (42528).
- 482 • Berthet MA, Angellier-Coussy H, Machado D, Hilliou L, Staebler A, Vicente A, Gontard
483 N. Exploring the potentialities of using lignocellulosic fibers derived from three food by-

- 484 products as constituents of biocomposites for food packaging. *Industrial Crops Products*,
485 2015; 69: 110–122.
- 486 • Berthet MA, Mayer-Laigle C, Rouau X, Gontard N, Angellier-Coussy H. Sorting natural
487 fibres: A way to better understand the role of fibre size polydispersity on the mechanical
488 properties of biocomposites. *Composites Part A*, 2017; 95: 12–21.
- 489 • Bishop PL, Godfrey C. Nitrogen transformations during sludge composting. *BioCycle*,
490 1983; 24: 34-39.
- 491 • Boopathy R. Factor limiting bioremediation technologies. *Bioresource Technology*,
492 2000;74: 63–67.
- 493 • Cardelli R, Benitez E. Changes of chemical properties in two soils amended with moist
494 olive residues. *Agricoltura Mediterranea*, 1998; 128: 171–177.
- 495 • Cardoso S M, Guyot S, Marnet N, da-Silva J A L, Renard CMGC, Coimbra MA.
496 Characterisation of phenolic extracts from olive pulp and olive pomace by electrospray
497 mass spectrometry. *Journal of the Science of Food and Agriculture*, 2005; 85:21–32.
498 DOI: 10.1002/jsfa.1925.
- 499 • Chevillard A, Angellier-Coussy H, Guillard V, Gontard N, Gastaldi E. Investigating the
500 biodegradation pattern of an ecofriendly pesticide delivery system based on wheat gluten
501 and organically modified montmorillonites. *Polymer Degradation and Stability*, 2012; 97:
502 2060-2068.
- 503 • Cooperband L. *The Art and Science of Composting: A Resource for Farmers and*
504 *Compost Producers*. University of Wisconsin-Madison, 2002.
- 505 • Dashtban M, Schraft H, Syed TA, Qin W. Fungal biodegradation and enzymatic
506 modification of lignin. Review Article. *International Journal of Biochemistry and*
507 *Molecular Biology*, 2010;1(1):36-50.

- 508 • De Bertoldi M, Vallini G, Pera A. The biology of composting: a review. waste manage
509 research,19831: 157-176.
- 510 • Dufresne A, Dupeyre D, Paillet M. Lignocellulosic flour-reinforced
511 poly(hydroxybutyrate-covalerate) composites. Journal of Applied Polymer Science,
512 2003;87: 1302.
- 513 • El-Hadi A, Schnabel R, Straube E, Müller G, Henning S. Correlation between degree of
514 crystallinity, morphology, glass temperature, mechanical properties and biodegradation of
515 poly(3-hydroxyalkanoate) PHAs and their blends. Polymer Testing, 2002; 21(6):665–674.
- 516 • Gharbi A, BelHassen R, Boufi S. Composite materials from unsaturated polyester resin
517 and olive nuts residue: The effect of silane treatment. Industrial Crops and Products, 2014;
518 62: 491–498.
- 519 • Gómez-Muñoz B, Hatch D J, Bol R, García-Ruiz R. The Compost of Olive Mill Pomace:
520 From a Waste to a Resource – Environmental Benefits of Its Application in Olive Oil
521 Groves. Chapter from the book Sustainable Development - Authoritative and Leading
522 Edge. Content for Environmental Management, 2012. <http://dx.doi.org/10.5772/48244>.
- 523 • Haddadin MSY, Haddadin Jb, Arabiyat OI, Hattar BA. Biological conversion of olive
524 pomace into compost by using *Trichoderma harzianum* and *Phanerochaete*
525 *chrysosporium*. Bioresource Technology, 2009;100: 4773–4782.
- 526 • Hassaini L, Kaci M, Touati N, Pillin I, Kervoelen A, Bruzard S. Valorization of olive
527 husk flour as a filler for biocomposites based on poly(3-hydroxybutyrate-co-3-
528 hydroxyvalerate): Effects of silane treatment. Polymer Testing, 2017;59: 430-440.
- 529 • Kourmentza C, Plácido J, Venetsaneas N, Burniol-Figols A, Varrone C, Gavala HN, Reis
530 MAM. Recent Advances and Challenges towards Sustainable Polyhydroxyalkanoate
531 (PHA) Production: a review. Bioengineering, 2017; 4, 55. DOI:10.3390/bioengineering
532 4020055.

- 533 • Kumar S, Das PM, Rebecca LJ, Sharmila S. Isolation and identification of LDPE
534 degrading fungi from municipal solid waste. *Journal of Chemical and Pharmaceutical*
535 *Research*, 2013; 5(3): 78-81.
- 536 • Kuzyakov Y, Friedel JK, Stahr K. Review of mechanisms and quantification of priming
537 effects. *Soil Biology and Biochemistry*, 2000; 32: 1485-1498. DOI 10.1016/S0038-
538 0717(00)00084-5.
- 539 • Lammi S, Barakat A, Mayer-Laigle C, Djenane D, Gontard N, Angellier-Coussy H. Dry
540 fractionation of olive pomace as a sustainable process to produce fillers for biocomposites.
541 *Powder Technology*, 2018a; 326: 44–53. DOI.org/10.1016/j.powtec.2017.11.060.
- 542 • Lammi S, Le Moigne N, Djenane D, Gontard N, Angellier-Coussy H. Dry fractionation of
543 olive pomace for the development of food packaging biocomposites. *Industrial Crops and*
544 *Products*, 2018b; 120: 250-261. DOI.org/10.1016/j.indcrop.2018.04.052
- 545 • Madison LL, Huisman GW. Metabolic engineering of poly(3-hydroxyalkanoates): from
546 DNA to plastic. *Microbiology and Molecular Biology Reviews*, 1999; 63(1): 21–53.
- 547 • Mais U, Esteghlalian AR, Saddler JN, Mansfield SD. Enhancing the enzymatic hydrolysis
548 of cellulosic materials using simultaneous ball milling. *Applied Biochemistry and*
549 *Biotechnology*, 2002; 98:815-832.
- 550 • Mousavioun P, Halley PJ, Doherty WOS. Thermophysical properties and rheology of
551 PHB/lignin blends. *Industrial Crops and Products*, 2013;50: 270–275.
- 552 • Muktadirul Bari Chowdhury AKM, Akratos CS, Vayenas DV, Pavlou S. Olive mill waste
553 composting: A review. *International Biodeterioration & Biodegradation*, 2013;85: 108-
554 119.
- 555 • Niaounakis M, Halvadakis CP. *Olive-Mill Waste Management*, first ed. Typothito-George
556 Dardanos, Athens. 2004.

- 557 • Nicholson DJ, Leavitt AT, Francis RC. A three-stage klason method for more accurate
558 determinations of hardwood lignin content. *Cellulose Chemistry and Technology*, 2014;
559 48 (1-2): 53-59.
- 560 • NF EN 17033 : 2018, Plastiques — Films de paillage biodégradables thermoplastiques
561 pour utilisation en agriculture et horticulture — Exigences et méthodes d'essai
- 562 • Plackett DV, Holm VK, Johansen P, Ndoni S, Nielsen PV, Sipilainen-Malm T, Sodergard
563 A, Verstichel S. Characterization of L-poly lactide and L-poly lactide–polycaprolactone co-
564 polymer films for use in cheese-packaging applications. *Packaging Technology and*
565 *Science*, 2006; 19:1–24.
- 566 • Pushpadass HA, Weber RW, Dumais JJ, Hanna MA. Biodegradation characteristics of
567 starch–polystyrene loose-fill foams in a composting medium. *Bioresource Technology*,
568 2010; 101: 7258–7264.
- 569 • Ravindran R, Jaiswal AK. Exploitation of food industry waste for high-value products.
570 *Trends in Biotechnology*, 2016; 34: 58–69.
- 571 • Singh R, Kumar M, Mittal A, Mehta PK. Lignocellulolytic enzymes: Biomass to biofuel.
572 *International Journal of Advanced Research*, 2016; 4(10): 2175-2182. DOI:
573 10.21474/IJAR01/2039.
- 574 • Singh Saharan B, Grewal A, Kumar P. Biotechnological Production of
575 Polyhydroxyalkanoates: A Review on Trends and Latest Developments. *Chinese Journal*
576 *of Biology*, 2014: 1–18. <http://dx.doi.org/10.1155/2014/802984>.
- 577 • Stoleru E, Hitruc EG, Vasile C, Opric L. Biodegradation of poly(lactic acid)/chitosan
578 stratified composites in presence of the *Phanerochaete chrysosporium* fungus. *Polymer*
579 *Degradation and Stability*, 2017; 143: 118-129.

- 580 • Taherzadeh MJ, Karimi K. Pretreatment of Lignocellulosic Wastes to Improve Ethanol
581 and Biogas Production: A Review. *International Journal of Molecular Sciences*, 2008; 9:
582 1621-1651.
- 583 • Tokiwa Y, Calabia BP, Ugwu CU, Aiba S. Biodegradability of Plastics: *Review*.
584 *International Journal of Molecular Sciences*, 2009; 10: 3722-3742.
585 DOI:10.3390/ijms10093722.
- 586 • Wei L, Liang S, McDonald AG. Thermophysical properties and biodegradation behavior
587 of green composites made from polyhydroxybutyrate and potato peel waste fermentation
588 residue. *Industrial Crops and Products*, 2015; 69: 91–103.

Figure Captions.

Figure 1. Kinetic of biodegradation (A) and biodegradation rate (B) of OP-based fillers in sol.

Figure 2. SEM pictures of olive pomace-based fillers (scale bar = 300 μm).

Figure 3. Antibiofilm results of OP-based fillers and OP-based composites after incubation at 37°C during 24h.

Figure 4. Kinetic of biodegradation (A) and biodegradation rate (B) of OP/PHBV-based composites in sol.

Figure 5. SEM pictures of OP/PHBV-based biocomposites surfaces (x 500: scale bar = 60 μm , x 1000: scale bar = 30 μm).

Figures.

Figure 1.

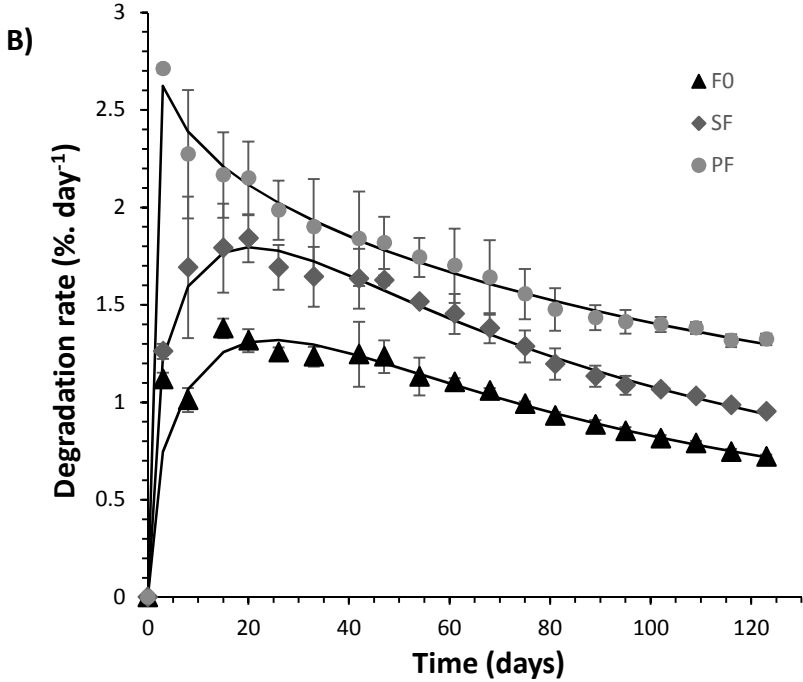
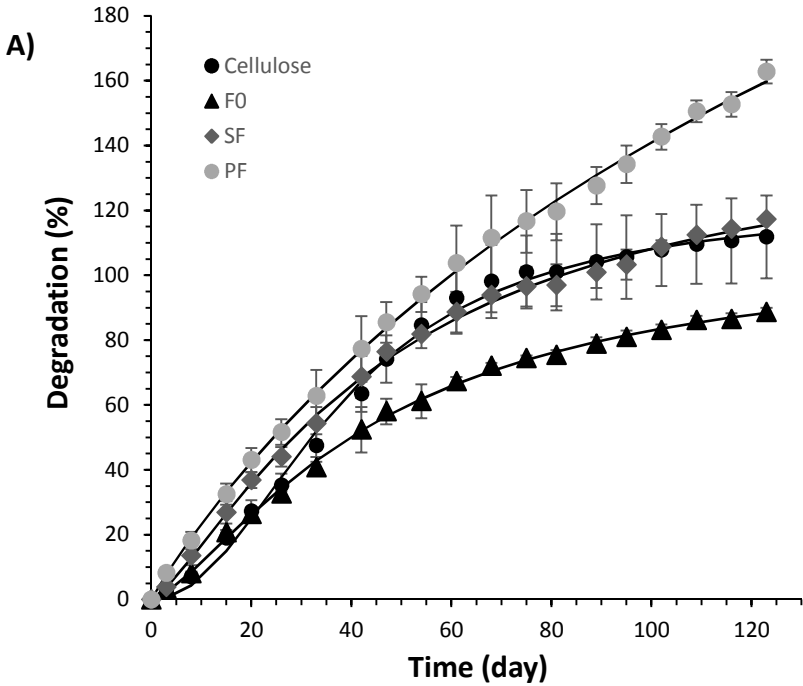


Figure 2.

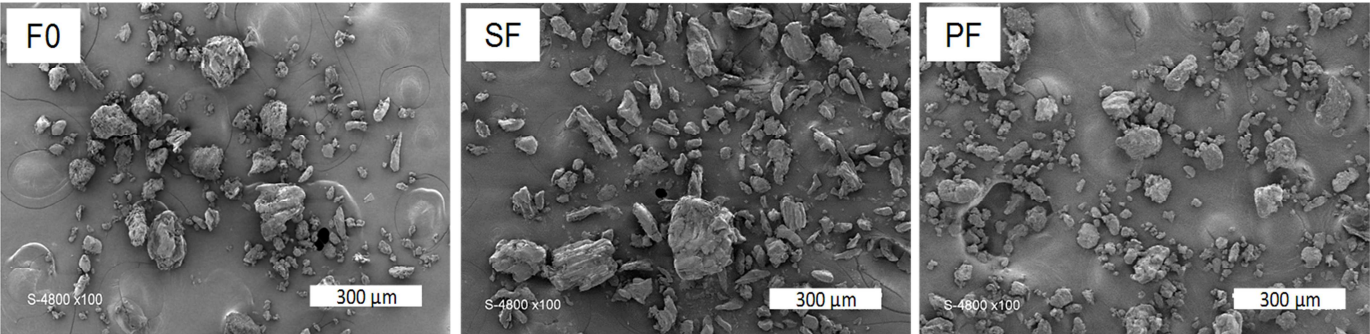


Figure 3.

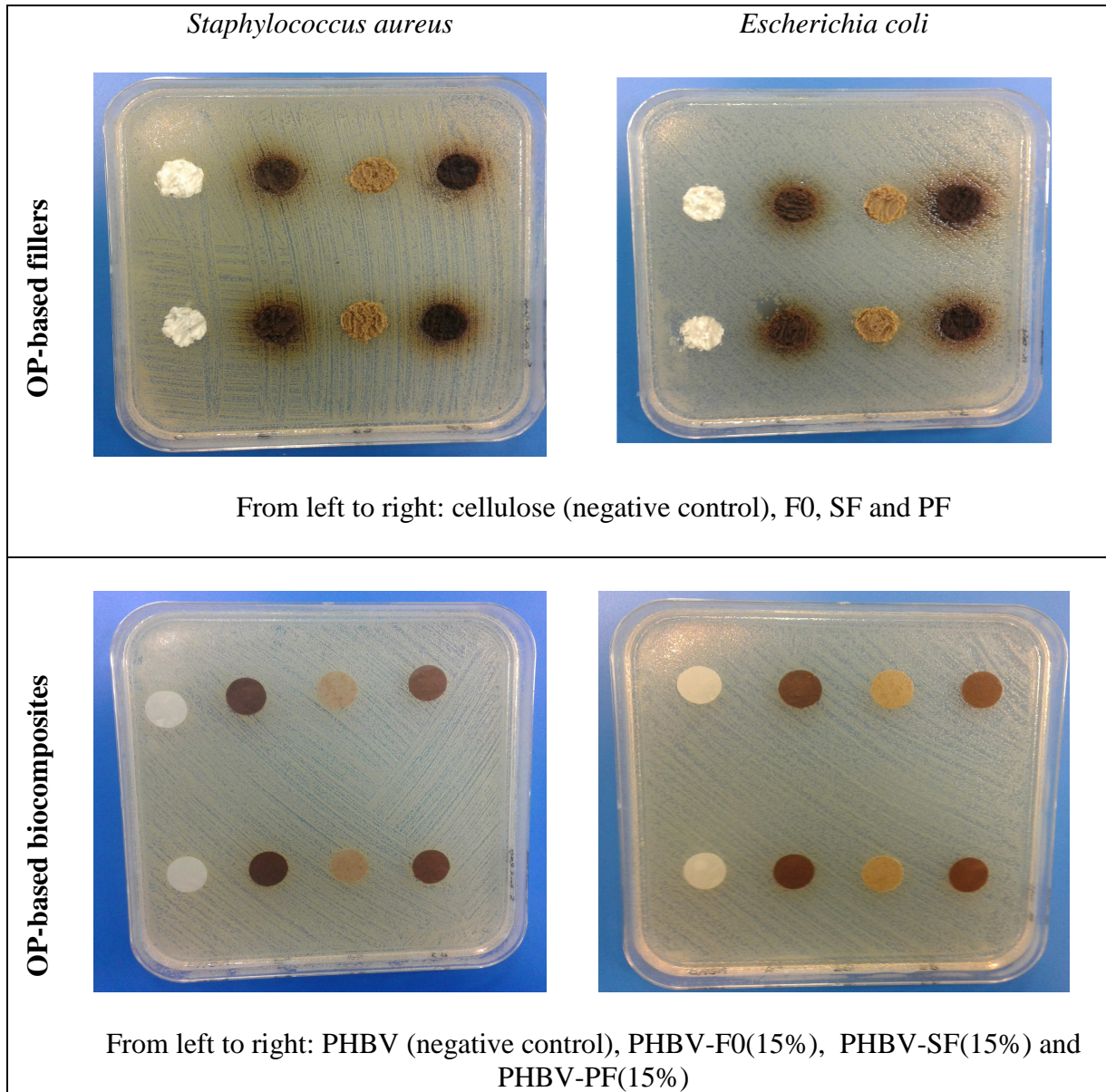


Figure 4.

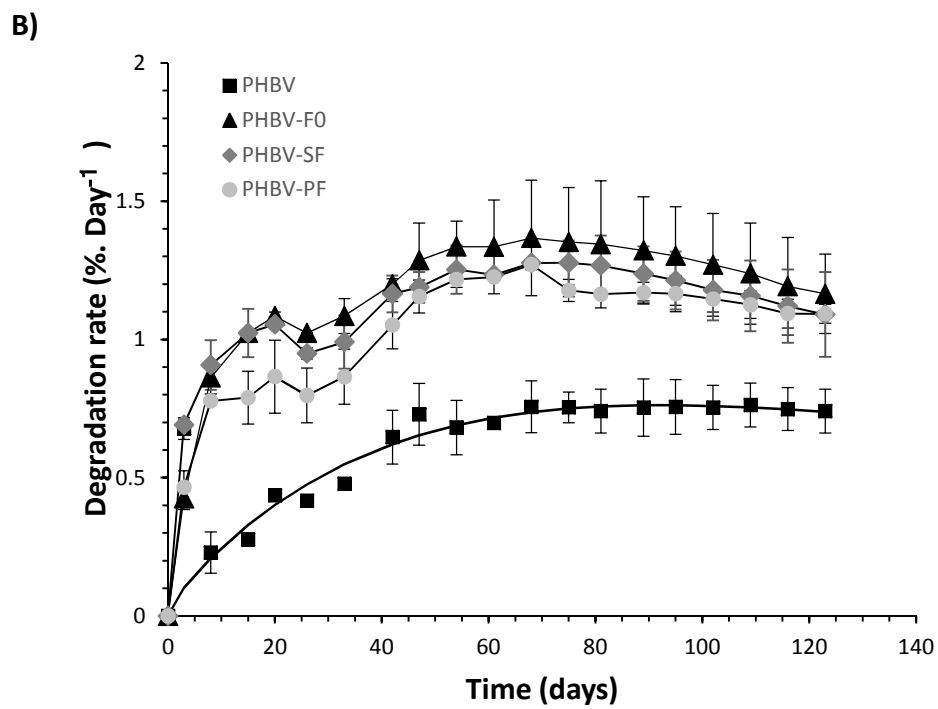
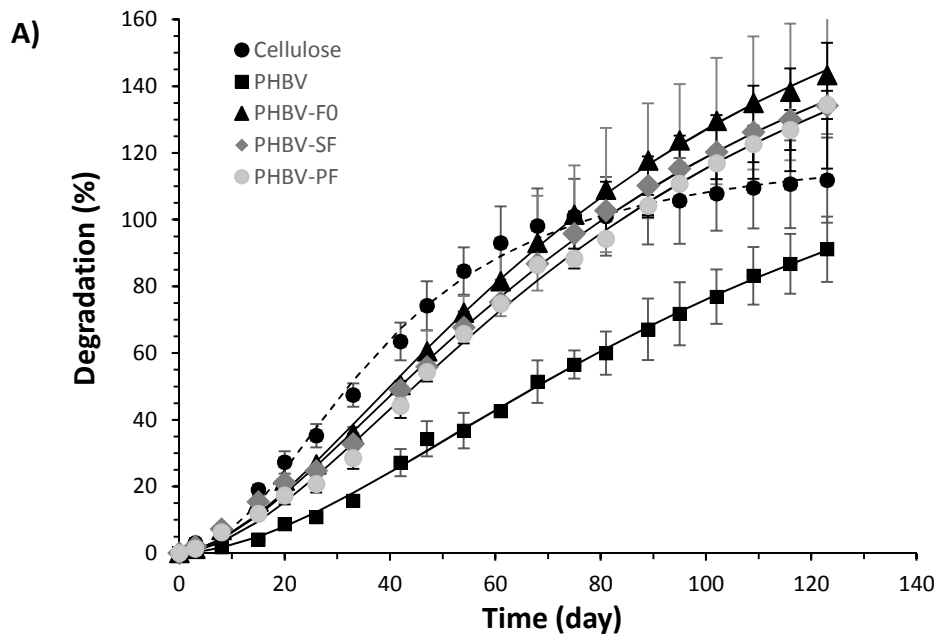
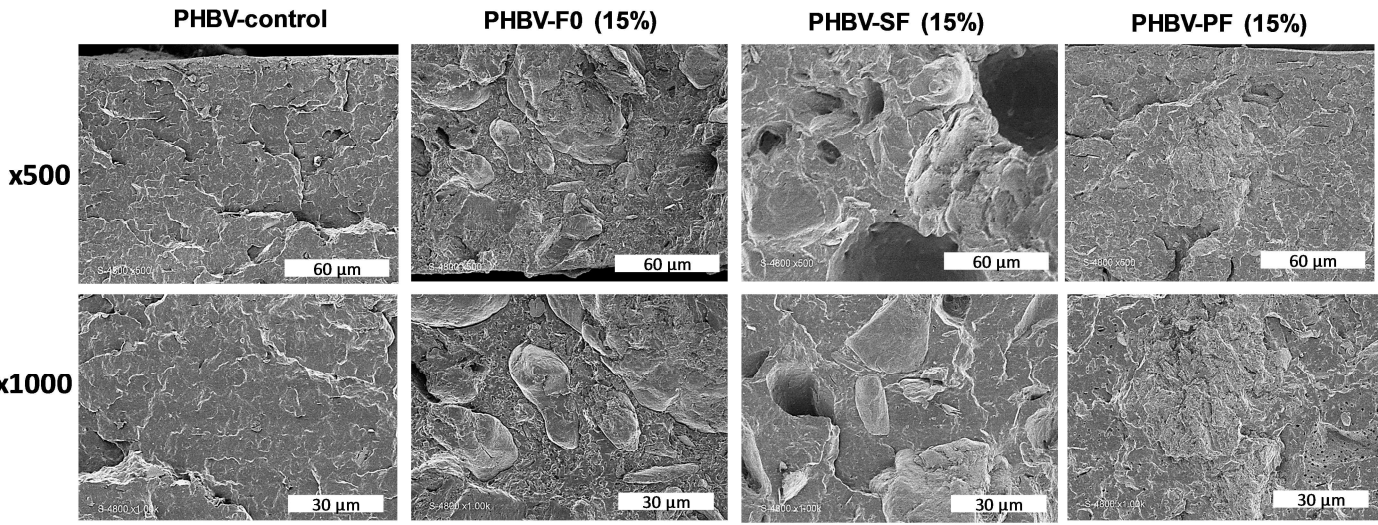


Figure 5.



Tables.

Table 1: Hill parameters (Deg_{max} , k , n) and related biodegradation indicators ($\text{Time}_{\text{rate max}}$, $\text{Deg}_{\text{rate max}}$) of OP-based fillers and OP/PHBV-based composites in respirometric test.

Sample	Hill parameters				$\text{Time}_{\text{rate max}}^{\text{b}}$ [days]	$\text{Deg}_{\text{rate max}}^{\text{c}}$ [% day ⁻¹]
	$\text{Deg}_{\text{max}}^{\text{a}}$ [%]	k [days]	n	R^2		
Control(cellulose)	122 (± 3.1)	38.2 (± 1.3)	2.1 (± 0.1)	0.99	42	1.6
F0	109 (± 3.0)	44.9 (± 2.1)	1.4 (± 0.0)	0.99	15	1.3
SF	147 (± 5.6)	46.7 (± 3.2)	1.3 (± 0.0)	0.99	20	1.8
PF	426 (± 66.5)	213.1 (± 60.9)	0.9 (± 0.0)	0.99	3	2.6
PHBV	163 (± 15.5)	108.2 (± 11.5)	1.7 (± 0.1)	0.99	95	0.7
PHBV-F0(15%)	219 (± 12.0)	82.6 (± 5.8)	1.7 (± 0.1)	0.99	68	1.3
PHBV-SF(15%)	209 (± 14.3)	84.9 (± 7.5)	1.6 (± 0.1)	0.99	68	1.3
PHBV-PF(15%)	204 (± 15.7)	85.6 (± 8.1)	1.7 (± 0.1)	0.99	68	1.2

Values in parentheses represent the confident intervals.

^a Deg_{max} : percentage of degradation at infinite time;

k : constant of the Hill equation representing the time for which $\text{Deg} = 1/2 \text{Deg}_{\text{max}}$;

n : constant of the Hill equation representing the curve radius of the sigmoid function.

^b $\text{Time}_{\text{rate max}}$: time to reach the maximum biodegradation rate.

^c $\text{Deg}_{\text{rate max}}$: maximum degradation rate.

Table 2: Biochemical composition (% dry basis) of olive pomace fractions

	Yield	pH	Humidity	Ashes	Cellulose	Hemicellulose	Lignin	Proteins	C	N
F0	100	4.9± 0.0	4.5± 0.0	2.6± 0.2	12.8±3.1	11.9±2.6	44.2±4.3	4.9	51.07	0.78
SF	56.4	4.9± 0.0	3.3± 0.0	0.8 ±0.0	17.4±1.1	18.5±0.4	37.7±3.4	0.6	49.97	0.09
PF	31.3	5.0± 0.0	7.2 ±0.0	4.6± 0.1	10.8±0.9	7.9±0.4	48.9±5.9	8.7	52.05	1.38